ISSN 1063-7826, Semiconductors, 2016, Vol. 50, No. 5, pp. 607–611. © Pleiades Publishing, Ltd., 2016.
Original Russian Text © A.S. Il'in, N.P. Fantina, M.N. Martyshov, P.A. Forsh, A.S. Chizhov, M.N. Rumyantseva, A.M. Gaskov, P.K. Kashkarov, 2016, published in Fizika i Tekhnika Poluprovodnikov, 2016, Vol. 50, No. 5, pp. 619–623.

SEMICONDUCTOR STRUCTURES, LOW-DIMENSIONAL SYSTEMS, AND QUANTUM PHENOMENA

Effect of Cadmium-Selenide Quantum Dots on the Conductivity and Photoconductivity of Nanocrystalline Indium Oxide

A. S. Il'in[a, b, c]*, N. P. Fantina[a], M. N. Martyshov[a, b], P. A. Forsh[a, b], A. S. Chizhov[d], M. N. Rumyantseva[d], A. M. Gaskov[d], and P. K. Kashkarov[a, b, c]

[a] *Faculty of Physics, Moscow State University, Moscow, 119991 Russia*
[b] *Russian Research Centre Kurchatov Institute, Moscow, 123182 Russia*
[c] *Moscow Institute of Physics and Technology, Dolgoprudnyi, Moscow oblast, 141700 Russia*
[d] *Faculty of Chemistry, Moscow State University, Moscow, 119991 Russia*
**e-mail: as.ilin@physics.msu.ru*

Submitted October 29, 2015; accepted for publication November 13, 2015

Abstract—The effect of cadmium-selenide quantum dots addition on the electrical and photoelectric properties of nanocrystalline indium oxide with nanocrystal dimensions in the range from 7 to 40 nm is studied. By impedance spectroscopy, it is shown that the addition of quantum dots substantially influences the resistance of interfaces between In_2O_3 crystals. A change in the character of the photoconductivity spectrum of In_2O_3 upon the addition of CdSe quantum dots is detected, and it is established that this change depends on the In_2O_3-nanocrystal dimensions. An energy band diagram is proposed to explain the observed change in the photoconductivity spectrum of In_2O_3 upon the addition of CdSe quantum dots.

DOI: 10.1134/S1063782616050110

1. INTRODUCTION

Due to a large specific surface area, nanocrystalline indium oxide (In_2O_3) can serve as the sensitive layer of resistive gas sensors. For example, indium oxide is sensitive to the presence of such gases as CO, NO, NO_2, O_3, etc. [1] in the atmosphere.

At present, gas sensors based on metal oxides operate, as a rule, under high-temperature (about 400°C), which causes considerable power consumption [2, 3]. In this context, studies in the field of the production of sensitive layers of low-temperature gas sensors are rather urgent. One of the lines of investigations in this field is the study of the effect of illumination on the properties of nanocrystalline In_2O_3 and analysis of the possibilities of detecting gases at room temperature by means of the illumination of In_2O_3 instead of heating [4, 5]. However, indium oxide is a wide-gap semiconductor [6] and practically transparent in the visible spectral region [7]. Therefore, the use of visible light for illumination is problematic. It is known that the photosensitivity can be improved by using various photosensitizers. The materials convenient for use as photosensitizers are colloidal semiconductor crystals or quantum dots (QDs). To date, the synthesis of CdSe QDs, whose typical dimensions are 2–10 nm, has been adequately developed. The photoluminescence spectrum of such QDs lies in the visible region. At the same time, the question of how the addition of CdSe QDs influences the electrical and photoelectric properties of nanocrystalline In_2O_3 remains unclear, although the possibility of photosensitizing other metal oxides (ZnO, SnO_2, TiO_2) with colloidal CdSe QDs has already been studied [8–10]. The studies presented below are devoted to answering the above question. It is also worth noting that the electrical and photoelectric properties of nanocrystalline indium oxide heavily depend on the nanocrystal size [11, 12]. Therefore, in this study, we analyze the effect of CdSe QDs addition on the properties of In_2O_3 with nanocrystals of different sizes.

2. EXPERIMENTAL

The nanocrystalline indium–oxide samples to be studied were produced by the sol–gel technique. The method of fabrication of the samples and their structure are described in more detail elsewhere [13]. We studied two series of nanocrystalline indium-oxide samples; cadmium-selenide QDs were added to one of the series. The CdSe QD size was 2–3 nm. Each of the series included three nanocrystalline In_2O_3 samples, in which the nanocrystals were different in size (7–8, 17, and 40 nm). Table 1 lists the notation of the samples and some of their structural parameters.

To perform electrical and photoelectric measurements, we deposited gold contacts onto the sample surfaces. Measurements were conducted in the temperature range 270–470 K. To study the electrical

Table 1. Notation and structure of samples

Sample	Nanocrystal size, nm	Presence of QDs
Sample *1*	7–8	No
Sample *2*	17	No
Sample *3*	40	No
Sample *1'*	7–8	CdSe
Sample *2'*	17	No
Sample *3'*	40	No

Table 2. Parameters of the equivalent circuit for all samples

	Sample *1*	Sample *1'*	Sample *2*	Sample *2'*	Sample *3*	Sample *3'*
R_1, kΩ	0.58	0.1	0.15	0.08	0.46	0.26
R_2, kΩ	322.1	19.0	20.8	9.7	0.6	2.2
C_2, pF	6.2	5.3	4.8	4.1	4.1	34.6

properties of nanocrystalline In_2O_3 by impedance spectroscopy, we used an HP 4192A impedance analyzer. To study the photoconductivity spectra, we used a system that included a DKSL-1000 xenon lamp and an MDR-12 grating monochromator. The intensity of light incident on the sample was 5 mW cm^{-2}. The photoconductivity (σ_{ph}) was determined as the difference between the conductivity of the sample upon illumination and the dark conductivity (σ).

3. RESULTS AND DISCUSSION

The temperature dependences of the dark conductivity of nanocrystalline In_2O_3 samples with and without CdSe QDs are shown in Fig. 1. It can be seen that the addition of CdSe QDs differently influences the conductivity of the nanocrystalline In_2O_3 samples with different average nanocrystal dimensions. The conductivity of nanocrystalline In_2O_3 samples with the smallest nanocrystal dimensions (7–8 nm) among those studied is significantly increased upon the addition of CdSe QDs. At the same time, the changes in the conductivity of nanocrystalline In_2O_3 samples with a larger average size are not so substantial; moreover, the dark conductivity of the sample with the largest average nanocrystal size becomes even lower upon the addition of CdSe QDs.

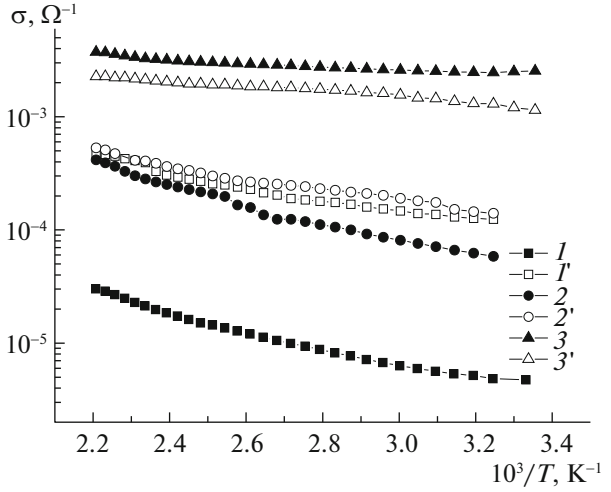

Fig. 1. Temperature dependences of the conductivity of In_2O_3 samples with different nanocrystal dimensions.

To clarify the causes of the experimentally observed changes, we studied the frequency dependences of the conductivity of the samples. Figure 2 shows the hodographs (the imaginary part of the impedance versus the real part) for samples *1* and *1'*. Similar hodographs were also obtained for other samples. The hodographs shown in Fig. 2 can be described by the equivalent circuit presented in panel (a). The circuit consists of a parallel *RC* circuit with additional resistance connected in series to the *RC* circuit. For heterogeneous systems, it is commonly thought [14] that the resistance R_1 is the resistance of the nanocrystal bulk and R_2 and C_2 are, correspondingly, the resistance and capacitance of the interfaces between nanocrystals. Approximations of the hodographs obtained for samples *1* and *1'* are shown in Fig. 2. The parameters of the equivalent circuit (R_1, R_2, C_2) for all of the samples under study are given in Table 2.

The impedance of the equivalent circuit shown in the inset in Fig. 2a is determined by the formula

$$Z = R_1 + \left(\frac{1}{R_2} + i\omega C_2\right)^{-1} = R_1 + \frac{R_2}{1+(\omega C_2 R_2)^2} - i\frac{\omega C_2 R_2^2}{1+(\omega C_2 R_2)^2}.$$

Consequently, the conductivity is

$$\sigma(\omega) = \frac{l}{S}\mathrm{Re}(Y) = \frac{1}{S}\frac{\left(1+\frac{R_1}{R_2}\right) + R_1\omega^2 C_2^2}{\left(1+\frac{R_1}{R_2}\right)^2 + \omega^2 C_2^2 R_1^2}, \quad (1)$$

where l is the sample thickness and S is the contact area. From formula (1), it can be seen that, at $R_2 \gg R_1$, we can distinguish three characteristic portions of the frequency dependence of the conductivity $\sigma(\omega)$:

$$\text{(i)}\ \sigma(\omega) = \frac{1}{S}\frac{1}{R_2} \quad \text{at} \quad \omega(R_1R_2)^{0.5}C_2 \ll 1; \quad (2)$$

$$\text{(ii)}\ \sigma(\omega) = \frac{1}{S}\omega^2 R_1 C_2^2 \ \text{ at } \ \omega(R_1R_2)^{0.5}C_2 \gg 1 \ \text{ and } \ \omega R_1 C_2 \ll 1; \quad (3)$$

$$\text{(iii)}\ \sigma(\omega) = \frac{1}{S}\frac{1}{R_1} \quad \text{at} \quad \omega R_1 C_2 \gg 1. \quad (4)$$

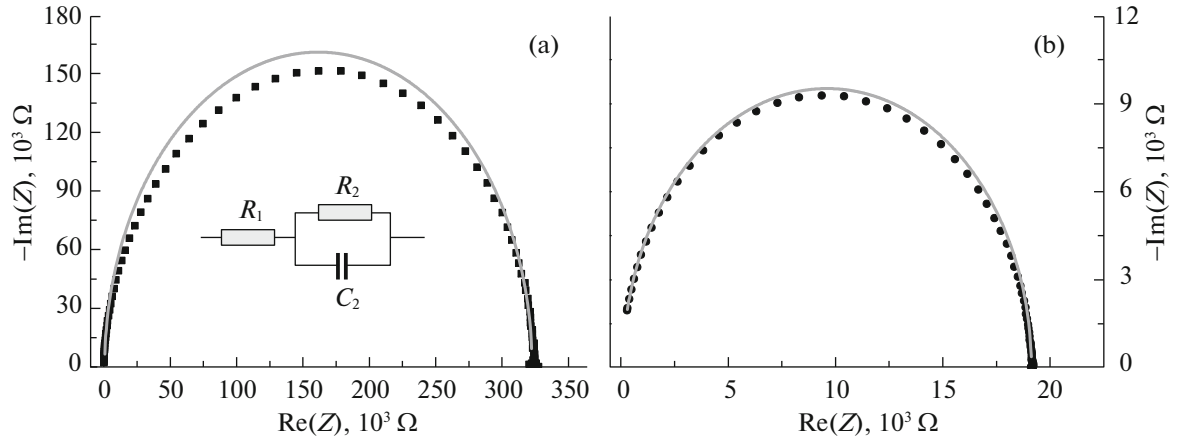

Fig. 2. Hodographs of the impedance of the samples (a) *1* and (b) *1'*. Solid lines show the approximation of the experimental data. Inset: the equivalent circuit.

Figure 3 shows the dependences of the conductivity of the samples on the ac signal frequency. From the dependences, it can be seen that, at frequencies below 1 MHz, the conductivity is practically independent of the ac signal frequency. At higher frequencies, the frequency dependence of the conductivity is close to a quadratic dependence. Thus, in the frequency region under consideration, the experimental dependences of the conductivity are in agreement with portions (i) and (ii) of the theoretical curve (formulas (2), (3)). To observe portion (iii) described by formula (4), we apparently need higher frequencies that cannot be attained with the impedance analyzer used in the experiment (the maximum attainable frequency was 13 MHz). It should be noted that similar frequency dependences of the conductivity are observed in nanostructured (porous) silicon [15, 16]. It can be anticipated that the behavior of the frequency dependence of the conductivity is defined by the nanocrystalline structure only and the addition of CdSe QDs does not modify the charge-carrier transport mechanism and induces only quantitative changes in the resistance.

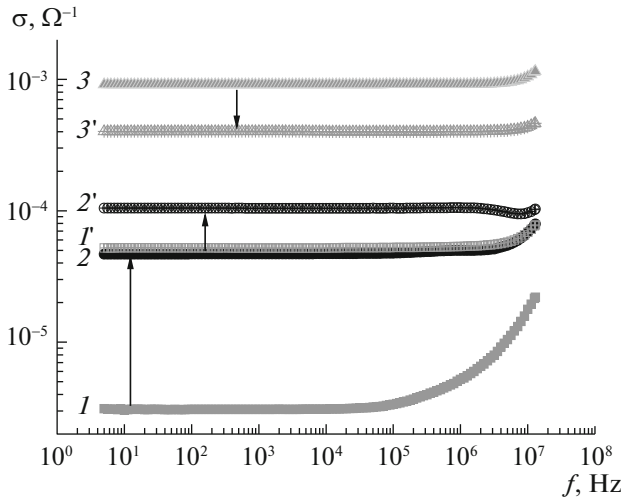

Fig. 3. Frequency dependences of the ac conductivity of the nanocrystalline In_2O_3 samples.

In addition, it should be noted that, as in the case of dc conductivity, the effect of CdSe QDs on the ac conductivity of In_2O_3 depends on the nanocrystal dimensions in the samples. Specifically, for sample *1*, we observe a significant increase in the conductivity upon the addition of CdSe QDs. At the same time, upon the addition of QDs, the conductivity of sample *2* changes more slightly, and in the case of sample *3*, the addition of CdSe QDs to the structure even leads to a decrease in the conductivity.

As follows from the equivalent circuit, the dc conductivity and the ac conductivity at low ac signal frequencies are defined mainly by the resistance R_2, i.e., the resistance of the intercrystallite bridges. On the one hand, the incorporation of CdSe QDs into the structure of nanocrystalline In_2O_3 brings about the creation of additional surface states, at which charge carriers are trapped; as a result, the charge-carrier concentration is reduced, which reduces the conductivity. On the other hand, CdSe QDs can close the gaps between nanocrystals (i.e., the QDs can serve as bridges between nanocrystals), thus reducing the resistance R_2; this yields an increase in the conductivity. Competition between the above-mentioned two processes can be responsible for the experimentally observed unsteady character of the change in the conductivity of In_2O_3 upon the addition of CdSe QDs.

In the case of samples with the smallest nanocrystal dimensions, the specific surface area is maximal, and consequently, there are a large number of gaps between nanocrystals. In this case, the latter process dominates over the former. As a result, upon the addition of CdSe QDs, the conductivity increases. As the

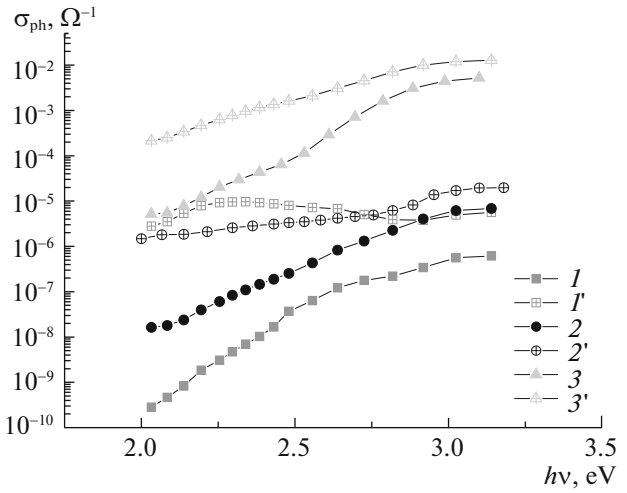

Fig. 4. Photoconductivity spectra of the nanocrystalline In_2O_3 samples.

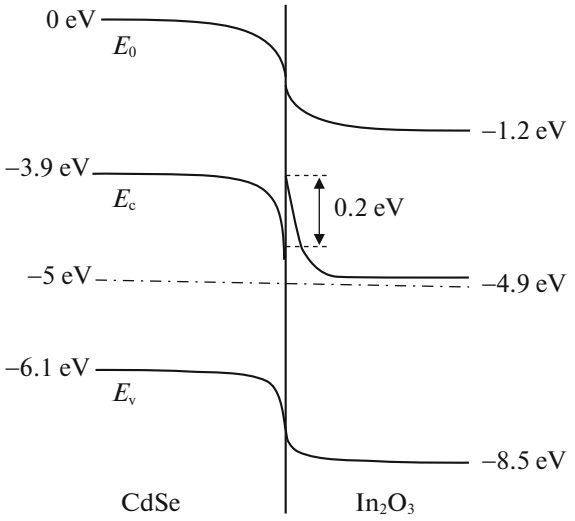

Fig. 5. Energy-band diagram of the In_2O_3/CdSe heterojunction. E_0 is the vacuum level, E_c is the bottom of the conduction band, and E_v is the top of the valence band.

nanocrystal size increases, the number of gaps becomes smaller and smaller, and the process of charge-carrier trapping at surface states formed upon the addition of CdSe QDs starts to dominate, resulting in a decrease in the conductivity.

To produce a sensor operating under conditions of additional illumination at room temperature, it is essential to gain information on the photoelectric properties of the material serving as the sensitive layer of the sensor.

Figure 4 shows the photoconductivity spectra of all of the nanocrystalline In_2O_3 samples under study. Except sample *1'*, all of the samples exhibit a maximum in the photoconductivity spectrum at the photon energy 3.2 eV. It can be conceived that, in this energy region, we observe interband absorption in nanocrystalline In_2O_3. At high photon energies, a decrease in the photoconductivity is observed. Since photons, whose energy exceeds the band gap, are absorbed mainly near the surface, the observed decrease in the photoconductivity can be attributed to the short lifetimes of nonequilibrium charge carriers in the surface layer of the semiconductor because of efficient surface recombination. It should be noted that the addition of CdSe QDs yields an increase in the photoconductivity in all of the samples in the visible spectral region (Fig. 4).

According to the data reported in publications [17, 18], the values of the electron affinity in CdSe and In_2O_3 are 3.9 and 3.7 eV, respectively. The band gap of CdSe is 2.2 eV, whereas the band gap of In_2O_3 is 3.6 eV. With regard to these values, we can construct the band diagram of the In_2O_3/CdSe heterojunction (Fig. 5).

Upon exposure of the In_2O_3/CdSe sample to green light, a portion of electrons from the valence band of CdSe transitions to the conduction band. In the conduction band at the In_2O_3/CdSe interface, there is a potential barrier 0.2 eV high. However, as can be seen from the band diagram shown in Fig. 5, the energy of most electrons excited in CdSe is high enough for electrons to overcome the barrier. It should be noted that the energy-band diagram of the heterojunction is shown without regard for the quantum-confinement effect in CdSe. Consideration for this effect will result in the appearance of a size-quantization level that will lie higher than the bottom of the conduction band of CdSe; therefore, it will be even easier for electrons to overcome the barrier. Electrons that have overcome the barrier transfer into In_2O_3, resulting in an increase in the photoconductivity of the sample. Since the sample with the smallest nanocrystal size exhibits the largest specific surface area, the number of incorporated CdSe QDs in such a sample is maximal. Due to the large number of CdSe QDs, the contribution of electrons excited in CdSe to the photoconductivity can be decisive. Such a situation is observed in sample *1'*, in which the photoconductivity maximum is reached in the range 2.2–2.3 eV. It should be noted that the above-described mechanism of improvement in the photosensitivity of In_2O_3 in the green spectral region through the addition of CdSe QDs is based on charge (electron) transfer. However, the mechanism of the photosensitization of In_2O_3 through the energy transfer from CdSe QDs to the In_2O_3 matrix and the excitation of electrons from local levels in the band gap of In_2O_3 [19] cannot be ruled out as well.

Thus, the addition of CdSe to nanocrystalline In_2O_3 yields an increase in the photoconductivity in the visible spectral region. This effect can be used in the production of In_2O_3-based sensors operating at

room temperature under conditions of additional illumination.

4. CONCLUSIONS

The electrical and photoelectric characteristics of nanocrystalline In_2O_3 and the change in these characteristic upon the addition of CdSe QDs are studied experimentally.

Specifically, the frequency dependences of the conductivity of In_2O_3 samples are analyzed. It is established that the effect of CdSe QDs on the conductivity of nanocrystalline In_2O_3 is heavily dependent on the nanocrystal dimensions. An equivalent circuit is proposed to approximate the hodographs of the impedance of the In_2O_3 samples, and qualitative interpretation of the experimentally observed change in the conductivity of nanocrystalline In_2O_3 upon the addition of CdSe QDs is provided.

It is also established that the addition of CdSe QDs noticeably increases the photoconductivity of nanocrystalline In_2O_3 in the green spectral region. An energy band diagram is proposed to interpret the observed increase in the photoconductivity and the possible mechanisms of the photosensitization of In_2O_3 with CdSe QDs are suggested.

ACKNOWLEDGMENTS

The study was supported by FASIE, project no. UMNIK 0020176, and the RFBR, project no. 15-03-03026.

REFERENCES

1. G. Eranna, B. C. Joshi, D. P. Runthala, and R. P. Gupta, Crit. Rev. Solid State Mater. Sci. **29**, 3 (2004).
2. A. Ayeshamariam, M. Bououdina, and C. Sanjeeviraja, Mater. Sci. Semicond. Process. **16**, 686 (2013).
3. G. Korottsenkov, Mater. Sci. Eng. B **139**, 1 (2007).
4. A. S. Il'in, N. P. Fantina, M. N. Martyshov, P. A. Forsh, A. S. Vorontsov, M. N. Rumyantseva, A. M. Gaskov, and P. K. Kashkarov, Tech. Phys. Lett. **41**, 863 (2015).
5. D. Zhang, C. Li, S. Han, X. Liu, T. Tang, W. Jin, and C. Zhou, Appl. Phys. A **77**, 163 (2003).
6. P. Erhart, A. Klein, R. Egdell, and K. Albe, Phys. Rev. B **75**, 153205 (2007).
7. O. Bierwagen, Semicond. Sci. Technol. **30**, 024001 (2015).
8. B. Carlson, K. Leschkies, E. S. Aydil, and X.-Y. Y. Zhu, J. Phys. Chem. C **112**, 8419 (2008).
9. V. Chakrapani, K. Tvrdy, and P. V. Kamat, J. Am. Chem. Soc. **132**, 1228 (2010).
10. C. Nasr, P. V. Kamat, and S. Hotchandani, J. Electroanal. Chem. **420**, 201 (1997).
11. E. A. Forsh, A. V. Marikutsa, M. N. Martyshov, P. A. Forsh, M. N. Rumyantseva, A. M. Gaskov, and P. K. Kashkarov, Nanotechnol. Russ. **7**, 164 (2012).
12. Xiaoqing Wang, Maofeng Zhang, Jinyun Liu, Tao Luo, and Yitai Qian, Sens. Actuators B **137**, 103 (2009).
13. E. A. Forsh, A. V. Marikutsa, M. N. Martyshov, P. A. Forsh, M. N. Rumyantseva, A. M. Gaskov, and P. K. Kashkarov, Thin Solid Films **558**, 320 (2014).
14. E. Barsoukov and J. R. Macdonald, *Impedance Spectroscopy Theory, Experiment, and Applications* (Wiley, Hoboken, New Jersey, 2005).
15. P. A. Forsh, M. N. Martyshov, V. Yu. Timoshenko, and P. K. Kashkarov, Semiconductors **40**, 471 (2006).
16. P. A. Forsh, L. A. Osminkina, V. Yu. Timoshenko, and P. K. Kashkarov, Semiconductors **38**, 603 (2004).
17. Kevin Tvrdy, P. A. Frantsuzov, and Prashant V. Kamat, Proc. Natl. Acad. Sci. **108**, 29 (2011).
18. A. Klein, Appl. Phys. Lett. **77**, 2009 (2000).
19. I. A. Akimov, Yu. A. Cherkasov, and M. I. Cherkashin, *Sensibilized Photoeffect* (Nauka, Moscow, 1980) [in Russian].

Translated by E. Smorgonskaya